

Design and Development of Sertaconazole Nitrate Loaded Silver Nanoparticulate Mucoadhesive Tablets for the Treatment of Vaginal Candidiasis

Anuradha More¹, Sneha Shinde¹, Padmaja Kore¹, Vitthal Chopade¹, Atul Baravkar^{2*}, Jyoti Jawale³, Sonali Devne⁴, Rajanikant Kakade⁵, Nilesh Jadhav⁶, Avinash Tupe⁷, Abhay Hole²

¹*PES Modern College of Pharmacy, Nigdi, Pune, Maharashtra, India.

²ADT's School of Pharmacy & Research Centre, Baramati, Pune, India.

³Institute of Pharmaceutical Sciences & Research (For girls), Bhigwan, Pune, Maharashtra, India

⁴SGMSPM's Dnyanvilas College of Pharmacy, Pune, Maharashtra, India

⁵Siddhi College of Pharmacy, Murbad, Maharashtra, India

⁶Dr N J Poulbudhe College of Pharmacy, Ahmednagar, Maharashtra, India

⁷SVPM's College of Pharmacy, Malegaon, Baramati, Maharashtra, India

DOI: <https://doi.org/10.52783/tjjpt.v44.i2.127>

Abstract

Vaginal candidiasis, a fungal infection estimates that 75 % of women will be suffering at least once during their lifetime. The disorders of this infection might be premature birth, pelvic inflammation, abortion, the transmission of sexual disorders, etc. In the present research, mucoadhesive vaginal tablets containing sertaconazole nitrate-loaded silver nanoparticles formulations were developed which increases the proximity period of the medicine with the vaginal mucosa, showing sustained drug release. The drug-loaded silver nanoparticle was synthesized by the chemical reduction method. There was successful conjugation of sertaconazole nitrate with silver nanoparticles (Ser-AgNP1) therefore, the drug's solubility is increased by 2.51 folds. The confirmation of silver nanoparticles was accessed by UV-visible spectroscopy. The mucoadhesive vaginal tablets were formulated and evaluated for swelling index, mucoadhesive force, residence time, In vitro dissolution and release kinetics, stability, and antifungal study. Optimized batch F8 was selected based on optimum mucoadhesive force (2.59 ± 0.25 N), % swelling index (86.50 ± 0.11 %), and sustained drug release (95.63 ± 0.16 %) up to 12 hr and showed greater antifungal activity. Overall study reveals that a prepared novel formulation, a mucoadhesive vaginal tablet containing sertaconazole nitrate loaded silver nanoparticles prevail over sertaconazole nitrate poor solubility and delivered drug during an extended period of time and also improved antifungal activity against *Candida albicans*.

Keywords: Vaginal candidiasis, sertaconazole nitrate, silver nanoparticles, mucoadhesive vaginal tablet.

Introduction

"Vaginal candidiasis" is a mucosal contamination of the vagina essentially brought by the most prominent and common *Candida albicans* fungi because of its excellent mucus membrane binding ability [1,2]. Vaginal candidiasis is currently one of the most well-known conditions for which women need medical attention. Recurrence will affect 40 to 50% of them and chronic vaginal candidiasis will affect 5 to 8% of them [3,4]. Silver nanoparticles are scaled down to nanoscale sizes ranging from 1 to 100 nm they acquire high surface-to-volume ratios and exhibit characteristic properties of good chemical stability as well as broad-spectrum antifungal action due to their toxicity to fungi [5,6]. Additionally, silver nanoparticles often increase solubility, stability and reducing dose frequency of drug [7]. The silver nanoparticle can be formulated by the substance decrease strategy by utilizing sodium borohydride as a lessening specialist and chitosan as a stabilizer [8]. Chitosan is a naturally occurring polysaccharide with excellent biocompatibility, lower toxicity, and good

stabilizing properties along with better antifungal activity [9]. The surface science of silver nanoparticles, including their charge, phase of agglomeration, and antifungal spectrum, can be altered by the interaction of chitosan with silver nanoparticles [10].

Sertaconazole Nitrate (SRN) is (BCS class II) lipophilic, broad-spectrum third-generation antifungal imidazole ring derivative endowed with potent fungicidal and fungistatic activity. Effective against pathogenic yeast (*Candida albicans*, *Pityrosporum orbiculare*, *C. tropicalis*, dermatophytes (*Epidermophyton*). For the therapy of skin and mucosa mycoses, for example genital, dermal, and vocal candida infections. Minimum inhibitory concentration (MIC) value at which 90% culture are inhibited (MIC90) for SRN were $\leq 0.1-5$ ug/ml and for fungicidal activity value is $0.5-64$ ug/ml [11,12,13]. The vaginal route of administration is currently receiving more attention. Most conventional vaginal formulations have a number of drawbacks, including leakage, and low retention of the vaginal epithelium, which leads to poor patient compliance. So to circumvent these challenges local mucoadhesive vaginal drug delivery systems are being propagated [14]. The major benefit of mucoadhesive tablets are the release of drugs in a sustained manner and the plausibility of keeping up with them in the vaginal tract for an postponed period of time. They additionally empower lower dosing frequencies [15]. The current research work aimed to form silver nanoparticles with SRN and stabilize them with chitosan, thereby determining their synergistic effect and improved antifungal activity against *Candida albicans* fungi also might prevail over SRN poor solubility and develop mucoadhesive vaginal tablet containing SRN loaded silver nanoparticles skilled to convey drug during a lengthy timeframe productively, i.e. show sustained drug delivery using a combination of mucoadhesive polymers for local treatment of vaginal candidiasis.

Materials & Methods

Materials

Sertaconazole Nitrate (Optrix Laboratories Private Limited, Telangana, India), silver nitrate (Merk chemicals Mumbai), sodium borohydride, chitosan (degree of deacetylation >70%), hydroxypropyl methylcellulose K15M and guar gum (Research-Lab Fine Chem Industries, Mumbai), magnesium stearate (Hexon Laboratories Pvt. Ltd, Pune), microcrystalline cellulose (Milton Chemicals, Mumbai), glacial acetic acid (99.5%) (Loba Chemicals, Mumbai), methanol (Merk Life Science Pvt. Ltd, Mumbai), Agar powder and Nutrient broth (Sisco Research Laboratory Pvt. Ltd Mumbai) and dual processed water was utilized all through the experiment. Microorganism, *Candida albicans* (MTCC 4748) was taken from the Modern college of pharmacy, Nigdi, Pune-44.

Methods

Synthesis of Sertaconazole nitrate-loaded silver nanoparticle (Ser-AgNPs).

Synthesis of silver nanoparticles (AgNPs) by chemical reduction method.

AgNP1 was synthesized according to the technique portrayed by Pansara et al for certain adjustments [16]. In which, double distilled water was used to prepare one volume of AgNO_3 (3.84 mM) solution and one volume of NaBH_4 solution. NaBH_4 was maintained at a temperature below 5°C . One volume of AgNO_3 (3.84 mM) solution was stirred using a magnetic stirrer (300 rpm) at 25°C . A twofold volume of chitosan solution in glacial acetic acid with different focuses ($0.2 - 1001$ ug/ml) was appended to AgNO_3 solution followed by one volume of NaBH_4 solution. The solution was mixed consistently for 10-15 min to obtain a yellow-colored solution.

The last engrossment of silver was 0.96 mM (101 mg/ml). To get AgNP1, the concentration of AgNO_3 was fixed at 0.96 mM, the concentration of chitosan varied from 0.1 to 501 ug/ml and NaBH_4 concentrations were equal to (1:1), double (1:2), and four-time (1:4) the concentration of AgNO_3 . After the appropriate chitosan and NaBH_4 solution concentration for AgNP1 synthesis were determined. Other chitosan stabilized silver nanoparticles (AgNP2, AgNP3, AgNP4, AgNP5) were synthesized with appropriate concentration ratios listed in (Table 1).

Table 1. Concentration of reactants of AgNPs

Sample	AgNO_3 (mM)	Chitosan (ug/ml)	NaBH_4 (mM)
AgNP1	0.96	101	1.92
AgNP2	1.92	201	3.34
AgNP3	2.88	301	5.76
AgNP4	3.84	401	7.68
AgNP5	5.00	501	10.00

Characterization of silver nanoparticles (AgNPs).

UV- Visible spectroscopy

The synthesized AgNPs were analyzed using (Shimadzu UV-1800, Japan) UV- spectrophotometer. The sweep

range was set from 200 to 700nm. The most extreme absorbance crest gives the preliminary confirmation of the presence of silver nanoparticles [5]. The detection was carried out in triplicate.

Loading of SRN onto silver nanoparticles (Ser-AgNPs)

SRN solution (10mg/ml methanol) was added drop by drop to the dispersion of silver nanoparticles, composition shown in Table no 3 and named Ser-AgNP1 to Ser-AgNP5 [17]. The mixture of SRN and silver nanoparticle solution was then kept for continuous stirring for 2 h at room temperature and was lyophilized for further use.

Characterization of SRN-loaded silver nanoparticles (Ser-AgNPs).

Particle size, polydispersibility index and zeta potential determination

Molecule size and zeta potential were determined by using particle size analyzer and zeta analyzer (Horiba nano analyzer & SZ-100). The AgNPs solution of 1 ml was diluted into 10 ml double distilled water under delicate blending in a glass container. One ml aliquot was removed and was set in a polystyrene cuvette way length 1 cm which was put in a thermoregulator maintained at 25°C. Detection was carried out in triplicate at a scattering angle of 90°. The polydispersity index (PDI) was determined in triplicate using photon correlation spectroscopy with an in-built zeta analyzer (Horiba nano analyzer & SZ-100) [18].

Drug Loading Efficiency

The resulting Ser-AgNps solution was centrifuged at 10,000 rpm for 60 minutes using the centrifuge machine (Remi & R-8C). The pellets obtained were separated from supernatant solution and redispersed in methanol for additional portrayal. The free medication present in the floatable liquid was analyzed by UV-Visible spectroscopy (Shimadzu UV-1800, Japan). Surface adsorption of SRN on the silver nanoparticles was found by measuring the amount of free drug present in the supernatant. The drug stacking proficiency of nanoparticles is determined by utilizing the following formula [19].

$$\text{Loading efficiency (\%)} = \frac{\text{Total amount of Drug} - \text{Free drug}}{\text{The total amount of AgNPs}} \times 100$$

Saturation Solubility study

The shake flask method was used to measure saturation solubility. The SRN and an optimized sample of Ser-AgNP1 in overabundance amount were put independently in a glass stoppered volumetric jar containing 10 ml Phosphate buffer pH 4.5. The specimen was placed in an orbital extremity (Remi motors RIS-24BL) for 24 h at 37°C and 80 rpm for equilibration. The samples were filtered using Whatman filter paper and weakened suitably in phosphate buffer pH 4.5 and examined UV spectrophotometrically (SHIMADZU UV-1800, Japan) at 259.9 nm [20].

Fourier Transform Infra-Red Spectroscopy (FT-IR)

FTIR Spectra of pure SRN and Ser-AgNP1 were determined (Jasco, FTIR 4100) using the potassium bromide (KBr) dispersion method. Using dried KBr, the baseline correction was carried out. Prior to analysis, the KBr and samples were dehydrated in the oven for 30 min and completely blended in a glass mortar in a 1:300 (sample:KBr) ratio. These specimens were placed in a specimen holder and scanned over the wave number scale of 4000 to 400cm⁻¹ at an aspiration of 4 cm⁻¹ [21,22].

Differential Scanning Calorimetry (DSC)

DSC scans were recorded for pure SRN and Ser-AgNP1. Precisely weighed specimens (about 2-3 mg) were heated in thermally locked aluminium pan in the range of 30°C- 300°C under a consistent nitrogen stream of 40 ml/min at a heating rate of 10°C/min. As a reference, an empty aluminium pan was used [23].

Scanning Electron Microscopy (SEM)

The shape and surface morphological properties of pure SRN and Ser-AgNP1 were examined by SEM (JEOL JSM 6360A, India). The specimen for SEM was ready by daintily sprinkling powder on twofold sticky tape adhered to an aluminum stub which was then positioned in the filtering electron magnifying lens chamber and scanned [24]. Photomicrographs were taken at magnifications 100x and 1000x.

X-ray Diffraction (XRD)

The crystalline nature of pure SRN and Ser-AgNP1 was assured by an X-ray diffractometer (Bruker D8 advance). The sweep rate was 2 θ/min over a 2θ range of 0 to 40°C and with a time period of 0.02° [25].

Formulation of mucoadhesive vaginal tablets.

Method of formulation

Mucoadhesive vaginal tablets containing Ser-AgNP1 were formulated by direct pressure method using varying concentrations of different mucoadhesive polymers (HPMC K15M & Guar gum). Table 2 depicts the detailed composition of different mucoadhesive formulations. Mucoadhesive vaginal tablets were prepared by direct mixing the required quantities of drug, polymers and excipients and were gone through an 80 mesh sieve to obtain a homogenous mixture prior to compression. Finally, well-mixed powder was compressed using a single punch tablet compression machine (Cip D8 Lab press) fitted with round, flat-faced 12 mm punches [17]. Each tablet was containing equivalent to 300 mg of SRN and has an approximate weight of 800 mg. Nine batches were prepared and coded from F1-F9.

Table 2. Composition of different batches of mucoadhesive vaginal tablets.

Ingredient (mg)	F1	F2	F3	F4	F5	F6	F7	F8	F9
Ser-AgNP1	433.5 (Equivalent to 300 mg of SRN)								
HPMC K15M	200	-	100	100	200	100	50	100	75
Guar gum	-	200	100	200	100	50	100	75	100
croscryllinecellulose	158.5	158.5	158.5	58.5	58.5	208.5	208.5	183.5	183.5
Magnesium stearate	8	8	8	8	8	8	8	8	8
Total	800	800	800	800	800	800	800	800	800

(All quantities in mg) (Total weight of tablet- 800mg)

Evaluation of mucoadhesive vaginal tablets.

Pre-compression parameter

The drug, mucoadhesive polymer, and excipient were characterized by their micromeritics properties such as bulk density, tapped density, angle of repose, compressibility index, and Hausner's ratio [26] [27].

Post compression parameter

Physical characteristics of the formulated tablets

All prepared mucoadhesive tablets were characterized for their thickness, diameter, weight variation, hardness, and friability according to official methods. The thickness and diameter of the tablets were measured in mm by using the digital vernier caliper [28]. Ten tablets were randomly selected from each batch and averages were recorded [29]. As per USP thickness and diameter of the tablets should not exceed $\pm 5\%$ of a standard value [30]. From each batch, twenty tablets ($n=20$) were weighed individually using an electronic balanced, and their mean weight was determined [26]. The average weight of the tablet is more than 324 mg, hence 5% maximum difference is allowed as per USP [31]. The Monsanto hardness tester was used to determine the hardness of tablets [27]. The ten tablets from each batch were selected randomly and the value was reported in terms of kg/cm^2 [26] [32]. The friability of tablets was determined using Roche friabilator as per USP. Twenty tablets were weighed and kept in a Roche friabilator which was then driven for 100 revolutions (4 min) at a speed of 25 rpm [26].

Drug Content

The drug concentration of SRN in the prepared mucoadhesive vaginal tablets was found by UV spectrometry. Ten tablets were randomly selected from each batch and were weighed and crushed in mortar and powder corresponding to 100 mg of SRN was weighed and shifted to a 100 ml volumetric flask, volume was adjusted with methanol. The sample was filtered and the absorbance of the obtained solution was measured at a wavelength of 259.6 nm using a UV-Visible spectrophotometer (Shimadzu UV-1800, Japan) [27].

Determination of surface pH of tablet

The determination of surface pH was done by using a combined glass electrode. The tablet ($n=3$) from each batch was allowed to swell separately by exposing the tablet to 10 ml of phosphate buffer with a pH of 4.5 for 2 hrs at room temperature. The pH was measured by placing the electrode in close proximity to the outer plane of the tablets and permitting it to counterbalance for one minute [33].

Swelling Index

The swelling index of all batches was determined by using three tablets from each set. These tablets were separately weighed (W_0) and placed individually in petri dishes containing 30 ml of phosphate buffer pH 4.5 solution at $37 \pm 0.1^\circ\text{C}$. At regular intervals (1, 2, 3 up to 8h), the tablets were removed from the Petri dishes and tenderly tapped with channel paper to eliminate the overabundance water on the surface of the tablets [27]. The swollen tablets were reweighed and were noted (W_t) accordingly. The percentage of swelling was determined for

each tablet using the following formula [34]

$$\% \text{ Swelling Index (S.I)} = \frac{(W_t - W_o)}{W_o} \times 100$$

Where W_t is the weight of the tablet at time t and W_o is the initial weight of the tablet.

Ex vivo mucoadhesion time

The ex-vivo mucoadhesion time was evaluated after the application of mucoadhesive. Vaginal tablet on freshly cut in 3×3 cm squared pieces vaginal mucosal membrane of goat[35]. The fresh vaginal mucosal membrane was tied to the glass slide, and a mucoadhesivetablet was moistened with 1 drop of phosphate buffer from one side and pasted to the vaginal mucosal membrane by applying a light force with a fingertip for 30 seconds [18]. The glassslide was then vertically tied to the paddle of the dissolution apparatus, and placed in the dissolution bowl, which was filled with 250 ml of the phosphate buffer pH 4.5 and was maintained at $37 \pm 1^\circ\text{C}$. A slow stirring rate was applied after 2 minutes, to simulate the vaginal cavity atmosphere, and tablet adhesion was recorded for 12 hours. The time required for the tablet to complete detachment from the vaginal mucosal membrane was considered as the mucoadhesion time [36].

Ex-vivo mucoadhesion study

A changed equilibrium technique was utilized for deciding the mucoadhesive strength of the tablets ($n=3$) from each batch. The piece of the vaginal mucosal membrane was tied to the lower glass vial and the glass vial was firmly fitted into a glass receptacle loaded up with phosphate buffer pH 4.5, at $37 \pm 1^\circ\text{C}$ so that it just touched the mucosal surface. The mucoadhesive vaginal tablet was stuck to the lower side of an upper vial (which is attached to the left side pan of weighing balance) with the help of bilayered adhesive [37, 33]. Different sides of the equilibrium were made equivalent before the review. The water (identical to weight) was added gradually with a mixture set (100 drops/min) to the right-hand dish until the tablet disconnected from the mucosal surface [38]. The total weight required to detach two vials (the tablet from the mucosal surface) was taken as a proportion of the mucoadhesive strength in grams. The power of grip was determined by utilizing the given formula [34].

In vitro dissolution study

The fresh goat vaginal mucosal membrane was tied to the glass slide, and a mucoadhesive tablet was moistened with 1 drop of phosphate buffer pH 4.5 from one side and pasted to the vaginal mucosal membrane then the glass slide was vertically tied to the paddle of dissolution apparatus, and placed in the dissolution bowl containing 900 ml of phosphate buffer pH 4.5 [26]. Two mls of aliquots were removed at every 1 hour interval till 12 hours were replaced with an equal volume of phosphate buffer pH 4.5 to maintain sink condition. UV spectrophotometer (Shimadzu UV-1800, Japan) was used to analyze at 259.9 nm.

Drug release kinetics

The kinetics of the drug release was determined by the model fitting method using PCP Disso V3 software [18]. Data obtained from in-vitro drug release test was plotted into various kinetic models like the first order, zero order, Matrix, and Korsmeyer-Peppas models in order to ascertain the rate and mechanism of drug release from the prepared mucoadhesive tablet batches [20]. The model with the most noteworthy connection coefficient among them was viewed as the best fit model for the specific detailing. The worth near 1 was viewed as the most favored one [18].

Fourier Transform Infra-Red Spectroscopy (FTIR)

FTIR Spectra of SRN with polymer (physical mixture) and final tablet formulation F8 were determined (Jasco, FTIR 4100) using the potassium bromide (KBr) dispersion method. Using dried KBr, the baseline correction was carried out. Prior to analysis, the KBr and samples were dried in the oven for 30 min and thoroughly mixed in a glass mortar in a 1:300 (sample: KBr) ratio. These samples were placed in a sample holder and scanned over the wave number range of 4000 to 400cm^{-1} at a resolution of 2 cm^{-1} [21].

Differential scanning calorimetry (DSC)

DSC scans were recorded for SRN with polymer (physical mixture) and final tablet formulation F8. Accurately weighed samples (about 2-3 mg) were heated in a thermally sealed aluminum pan in the range of 30°C - 300°C under a constant nitrogen flow of 40 ml/min at a heating rate of $10^\circ\text{C}/\text{min}$. As a reference, an empty aluminum pan was used [23]

Antifungal study

Antifungal activity study of selected formulations was conducted in Microbiology laboratory, Modern college of

pharmacy, Nigdi, pune. The well diffusion method was used to performed In-vitro antifungal study against *candida albicans* in nutrient agar medium. In sterilized nutrient agar an aliquot of 0.5 Mcfarland standard final concentration of *Candida albicans* was mixed. Then this suspension was accurately mixed and 25 ml of this suspension was poured into sterile petri plates under aseptic condition, and then petri plate allowed to cool and solidify [26]. Then the required wells were punched by using sterile 6 mm cork borer in seeded nutrient agar medium plates. Then antifungal activity for selected formulations like SRN drug, chitosan, silver nanoparticles, marketed vaginal suppository, marketed vaginal tablet and optimized mucoadhesive vaginal tablet F8 against *candida albicans*. After completing incubation period, the antifungal activity was determined by measuring zone of inhibition by using antibiotic zone reader and expressed in terms of average diameter of zone of inhibition in millimeter.

Stability study

As per ICH Q1A guidelines stability study of optimized formulation was carried out in dark at room temperature ($25\pm 2^\circ\text{C}$) and at accelerated condition ($40\pm 2^\circ\text{C}$ and $75\pm 5\%$ RH) by packing them in aluminum foil and sealed tightly for 3 months [39]. The stability chambers were placed at both room and accelerated condition, which mentioned earlier [40]. Physical stability was observed by evaluating % swelling index, mucoadhesive force (N), percent drug content and cumulative drug release (%) at 0 day, 1, 2, and 3 months of interval, during the stability studies.

Statistical Analysis

Statistical significance was evaluated using the student's t-test. All data was reported as mean \pm standard deviation (SD) with $p < 0.05$ considered statistically significant.

Result And Discussion

Analytical reports of Silver nanoparticles (AgNP)

UV-visible spectroscopy (UV)

The end of reaction and synthesis of silver nanoparticles are indicated by a color change in reaction solution from colourless to yellow shown in (Figure 1).

The absorption spectrum of prepared AgNPs (Table 3) showed distinct UV-visible absorption peaks in the range 401.5 ± 0.19 nm to 422.7 ± 0.21 nm. Maximum absorption wavelength of AgNPs was red shifted as increased in sizes of silver nanoparticles. There is a blue shift to the shorter wavelength due to the decrease in particle size as the concentration of reducing agent NaBH_4 decrease. It is deep rooted that surface plasmon retention maxima relies upon size and state of the metal nanoparticles [41]. For optimized AgNP1 absorption peaks observed at 401.5 ± 0.19 nm as shown in Figure 2.

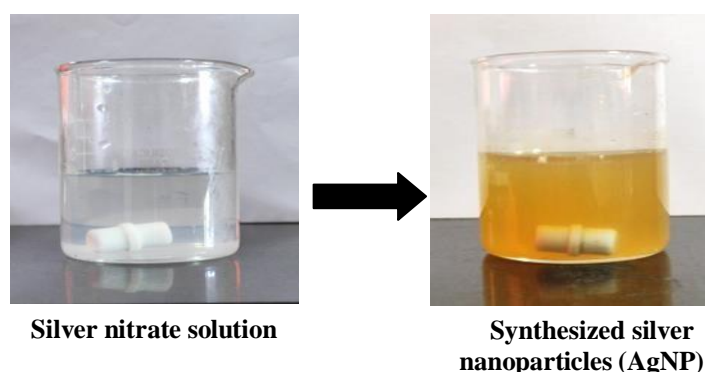


Figure 1. Color change reaction of silver nanoparticle synthesis.

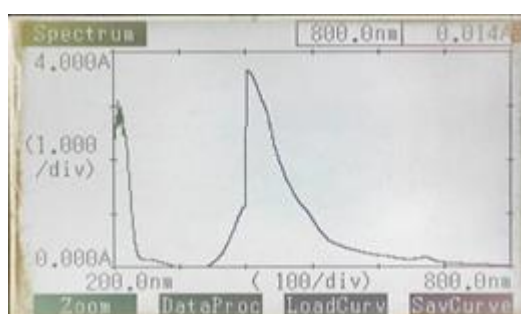


Figure 2. UV-visible absorption spectra of optimized sample of silver nanoparticle (AgNP1).
SRN loaded silver nanoparticles (Ser-AgNPs)

Particle size, Polydispersity index and Zeta potential

The particle size of drug loaded AgNP i.e. Ser-AgNP1 to Ser-AgNP5 was found to be in the range of 89.4 ± 0.24 nm to 182.2 ± 0.44 nm, PDI in the range of 0.474 ± 0.21 to 0.839 ± 0.38 and zeta potential in the range of 35.2 ± 0.18 to 30.76 ± 0.29 shown in Table 3. Figure 3 shows distinctive colours of Ser-AgNPs with different sizes and concentration of AgNO_3 , NaBH_4 , Chitosan. The stability of drug loaded AgNPs confirms with positive zeta potential value which might be due to amino functional groups of chitosan. The zeta potential values of Ser-AgNPs were beyond the limit -30mV , $+30\text{ mV}$ region, indicates all samples were stable in nature [42]. The optimized batch Ser-AgNP1 showed the particle size and polydispersity index and zeta potential 89.4 ± 0.24 , 0.474 ± 0.21 and 35.2 ± 0.18 respectively shown in (Figure 4) and (Figure 5) indicates sufficient distribution and low degree of a aggregation and highly stable dispersion of silver nanoparticle among other batches.

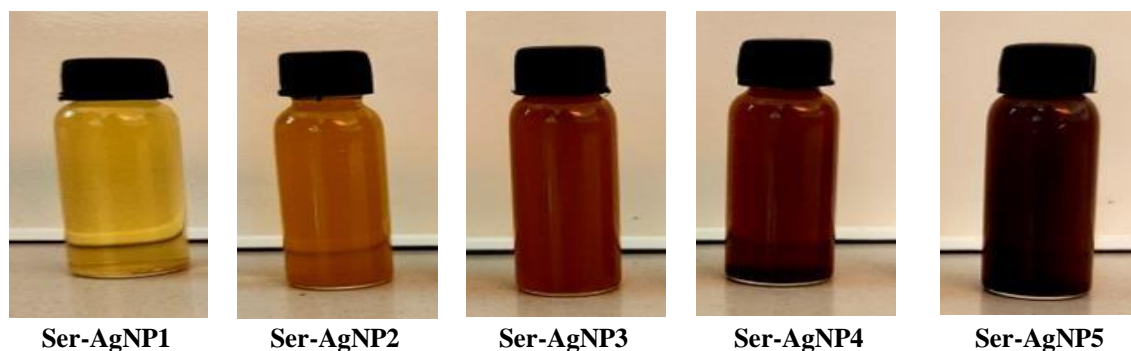


Figure 3. The distinctive colours of Ser-AgNPs with various particle sizes and concentrations.

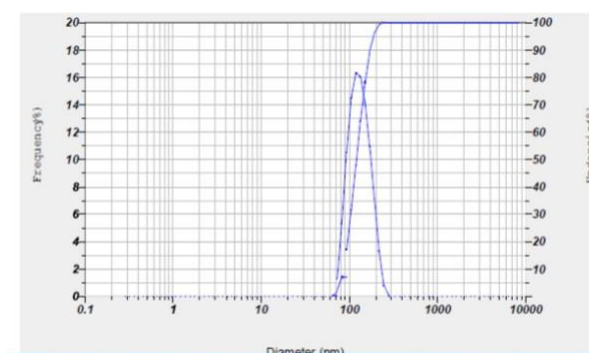


Figure 4. Particle size of optimized Ser-AgNP1.

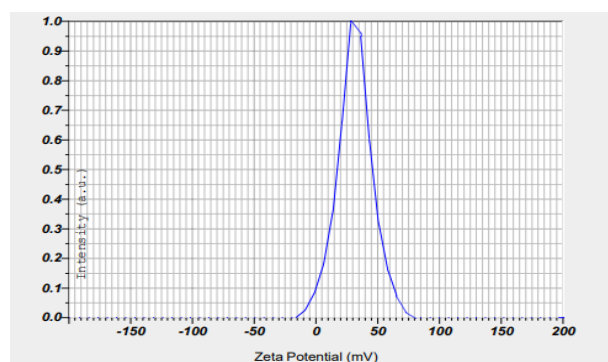


Figure 5. Zeta potential of optimized Ser-AgNP1

Drug Loading Efficiency (%)

The principle of drug loading on chitosan stabilized AgNPs is surface adsorption. If the increasing quantity of drug to silver nanoparticles decreases drug loading efficiency. So the optimized quantity of sertaconazole nitrate solution (i.e. 10 mg/ml methanol) was added to the AgNPs solution. The % drug loading capacity was found to be in the range ($97.7 \pm 0.37\%$ to $99.89 \pm 0.29\%$) for Ser-AgNP1 to Ser-AgNP5. The drug loading efficiency of optimized batch Ser-AgNP1 was found to be $98.76 \pm 0.25\%$ shown in Table 3.

Table 3. Characterization of SRN loaded silver nanoparticles (Ser-AgNPs)

Samples	Maximum absorbance peak (λ_{max})	Particle size (nm)	Zeta potential (mv)	Polydispersity index (PDI)	Drug loading efficiency (%)
Ser-AgNP1	401.5 ± 0.19	89.4 ± 0.24	35.2 ± 0.18	0.474 ± 0.21	98.76 ± 0.25
Ser-AgNP2	407.9 ± 0.33	116.5 ± 0.17	33.68 ± 0.24	0.681 ± 0.33	97.7 ± 0.37
Ser-AgNP3	415.3 ± 0.24	150.3 ± 0.23	33.03 ± 0.32	0.787 ± 0.30	98.5 ± 0.44
Ser-AgNP4	418.6 ± 0.42	170.9 ± 0.31	31.12 ± 0.31	0.756 ± 0.24	99.89 ± 0.29
Ser-AgNP5	422.7 ± 0.21	182.2 ± 0.44	30.76 ± 0.29	0.839 ± 0.38	99.85 ± 0.39

Saturation solubility study

The solubility of pure SRN in phosphate buffer pH 4.5 was found to be 9.2 ± 0.15 mcg/ml. But in the case of optimized Ser-AgNP1 the solubility increases by 2.51 folds i.e., 23.11 ± 0.24 mcg/ml, this might be due to a reduction in particle size in silver nanoparticles.

Optimized Ser-AgNP1 showed smaller particle size, and larger surface area, hence increasing the solubility, absorption rate, and bioavailability.

Fourier Transform Infra-Red Spectroscopy (FT-IR)

The FTIR spectra of SRN and optimized sample Ser-AgNP1 were evaluated (Figure 6, 7). From (Figure 6), it was found that the following peaks of the SRN are present in the IR graph of the standard and this confirms the quality of the drug [43]. The peaks were observed at 788.7 cm^{-1} , 2586.3 cm^{-1} due to C-Cl and S-H stretching which indicates that the original structure of SRN has been partly retained. The benzene ring present at 1560.13 cm^{-1} . The C-H, C=C, C=N, C-N stretch was observed at 2918.73 cm^{-1} , 1560.13 cm^{-1} , 1617.98 cm^{-1} , 1099.23 cm^{-1} . The C-O group was observed at 1384.6 cm^{-1} respectively. Figure 7 showed the IR of the Ser-AgNP1, the peaks of functional groups present in the drug were found to be within the range. Except the C-O group had a lower shift to 1024 & 1041 cm^{-1} , also there was a higher shift observed in C=N to 1657 cm^{-1} , this shift indicates that there must be the loading of SRN taking place on the silver. The peak 1344 cm^{-1} represents the residual nitrate ion. The bending vibration of NH_2 & stretching of C=O was observed at 1653 cm^{-1} which indicates the interaction between silver and the amino group of chitosan in the nanoparticle.

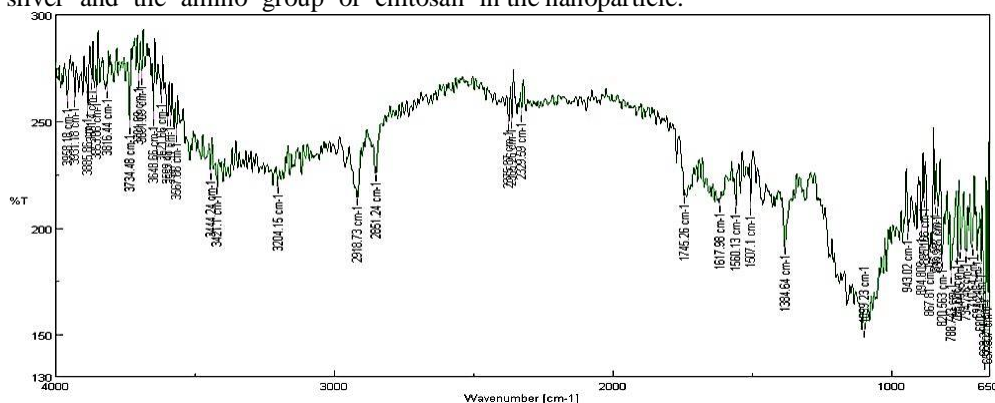


Figure 6. FT-IR spectroscopy of SRN.

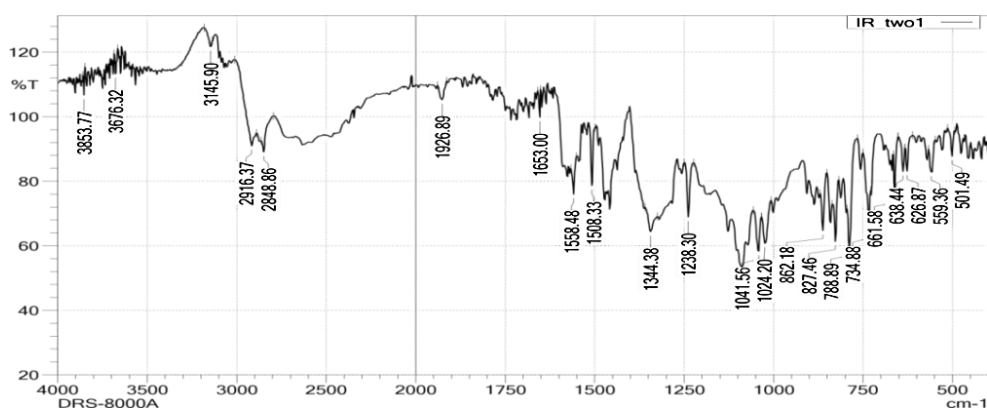


Figure 7. FT-IR spectroscopy of optimized Ser-AgNP1.

Differential scanning calorimetry (DSC)

DSC thermogram of SRN (Figure 8) shows the sharp endothermic peak at 161.55°C (reported value 156 - 157°C) [23]. The sharp endothermic peak in this region is due to the melting point of SRN. This sharpness of the peak determines the purity and crystalline nature of the drug. DSC thermogram of optimized Ser-AgNP1 (Figure 9) shows the endothermic peak firstly at 89.3°C (reported 90°C) [44]. Which determines the presence of the chitosan as this may be due to the melting point of chitosan. and the other moderately sharp endothermic peak (Figure 9) at temperature 168.6°C shows the presence of SRN loaded silver nanoparticles. In the DSC thermogram, SRN loaded silver nanoparticle (Ser-AgNP1) indicates that the drug exists in crystalline form.

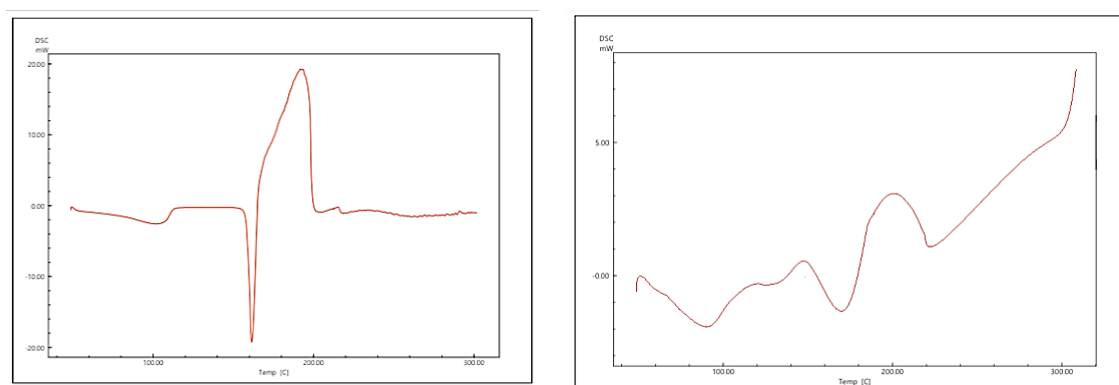


Figure 8. DSC thermogram of SRN & of optimized Ser-AgNP1.

Scanning Electron Microscopy (SEM)

Morphological characteristics of SRN and optimized Ser-AgNP1 were observed using SEM at magnification 100x and 1000x, as shown in (Figure 10), which revealed the irregular morphology with slight aggregation of Ser-AgNP1, which may be due to loading of the drug on AgNP. Whereas the morphology of pure SRN was rod shape.

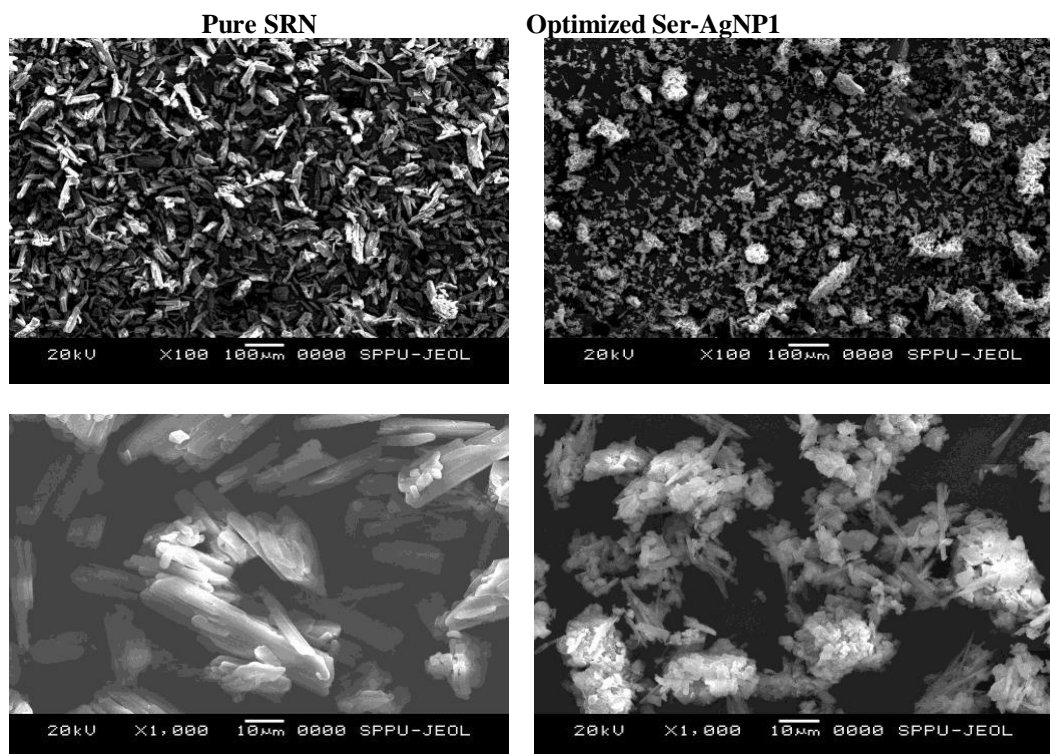


Figure 10. SEM images of pure SRN and optimized Ser-AgNP1 at magnification 100x and 1000x.

X-ray Diffraction (XRD)

The XRD pattern of SRN was shown in (Figure 11), with the following prominent peaks at 2θ (21.18° , 22.93° , 23.94° , 24.30° , 26.26° , 27.08° , 27.93° , 29.54° , 37.82°) are found at intensity (116, 397, 53, 589, 166, 136, 133, 135, 58 cps) respectively. Whereas the XRD pattern of optimized Ser-AgNP1 showed prominent peaks at 2θ (21.16° , 22.70° , 23.68° , 24.29° , 26.18° , 27.61° , 29.25° , 37.45°) are found at intensity (97, 158, 102, 327, 134, 50, 126, 47) respectively shown in (Figure 12). From this, it is indicated that the intensity of SRN gets moderately reduced in Ser-AgNP1. Also, Four Bragg's Reflections at 2θ of Ser-AgNP1 (38.88° , 45.89° , 54.74° , 59.63°) were corresponding to the (110, 202, 241, 311) plans. The result confirmed that Ser-AgNP1 was found in crystalline nanostructured and possessed face-centered cubic lattice [45].

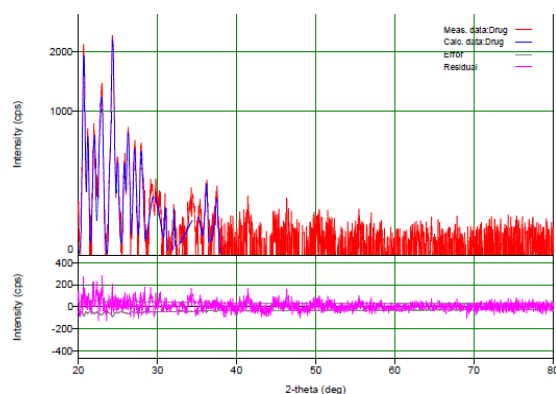


Figure 11. XRD pattern pure SRN.

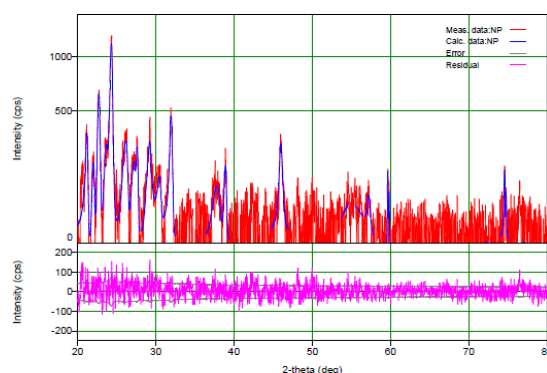


Figure 12. XRD pattern of optimized Ser-AgNP1.

Mucoadhesive vaginal tablets

Pre-compression parameters

Powder flowability fundamentally affects a few drug processes, including mixing, pressure, and dealing with [26]. Powder flowability was evaluated and characterized by USP grouping that all tried medication polymer mixes had either fair or acceptable flowability. The bulk density, tapped density, angle of repose, Hausner ratio, and compressibility index of formulation F1-F9 were found in the range of 0.50 ± 0.43 to 0.68 ± 0.37 g/ml, 0.59 ± 0.21 to 0.89 ± 0.34 g/ml, 30.7 ± 0.31 to 36.1 ± 0.28 , 1.18 ± 0.33 to 1.30 ± 0.25 and $16.4 \pm 0.22\%$ to $24.3 \pm 0.28\%$ respectively, which indicate all formulation showed fair or passable flowability. The bulk density, tapped density, angle of repose, Carr's compressibility index, and Hausner ratio for optimized formulation (F8) were found to be 0.62 ± 0.31 g/ml, 0.75 ± 0.22 g/ml, 30.7 ± 0.30 , $17.3 \pm 0.25\%$, 1.20 ± 0.35 respectively which indicate that optimized formulation (F8) exhibited fair flow properties.

Post compression parameter

Physical characteristics of the formulated tablets

Formulated mucoadhesive vaginal tablets containing SRN-loaded silver nanoparticles showed a round shape, light brown colored, and were odorless. Mathematical upsides of all the quality control boundaries, explored for F1-F9 different batches are depicted in (Table 4). Tablets thickness was almost uniform and found to be within the limit of deviation i.e. $\pm 5\%$ of the standard value. Also, the diameter was found to be uniform from 12 ± 0.31 to 12 ± 0.24 mm in all batches. In the hardness test, the hardness for different batches was found to be between 5.40 ± 0.35 to 6.13 ± 0.20 kg/cm². Similarly, the average percentage friability for all the formulations was between 0.30 ± 0.21 to $0.61 \pm 0.31\%$, which was within the acceptable range as mentioned in the USP i.e. underneath 1%, demonstrating that the tablets of all groups are having great minimization and showing sufficient protection from mechanical shock and scraped spot. In % weight variation study, the weight of the tablet varied between 796.2 ± 0.21 to 802 ± 0.30 mg which was within the USP limit i.e. more than 324 mg (5% deviation) of the respective average weight. The diameter, thickness, hardness, friability, and weight variation for optimized formulation (F8) were found to be 12 ± 0.16 , 4.99 ± 0.19 mm, 5.79 ± 0.21 kg/cm², $0.30 \pm 0.21\%$, 799.2 ± 0.20 mg respectively. All the formulations passed the evaluation tests and showed satisfactory results.

Drug Content

All the formulations F1-F9 pass the drug content test as per USP specification. The drug content of all the sets was found to be in the range of $96.42 \pm 0.30\%$ to $98.71 \pm 0.19\%$ respectively represented in (Table 4), which was within the limits and reflects good uniformity in drug content among different batches. The optimized batch F8 showed acceptable drug content uniformity i.e. $98.71 \pm 0.19\%$.

Surface pH

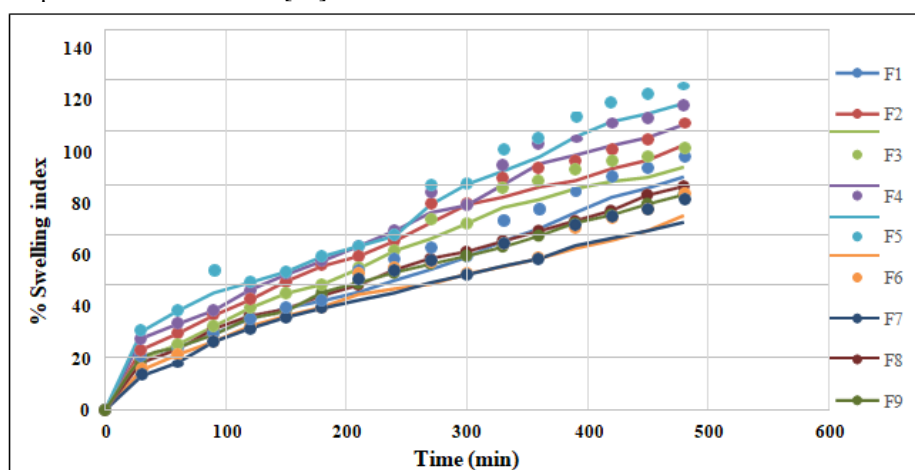
In order to investigate the possibility of any in vivo side effects, the surface pH of the tablet was determined. It was determined to maintain surface pH as close to the system pH of 4-4.5 as possible. Because an alkaline pH may cause irritation to vaginal mucosa [46]. The surface pH of all tablet formulations F1-F9 was found to be within the acceptable range of vaginal pH i.e. 4-4.5. Moreover, the surface pH of all the batches was in between 4.23 ± 0.38 to 4.50 ± 0.33 , thereby showing no vaginal mucosal irritancy and better patient compatibility. There was no impressive distinction in the surface pH of tablets. The surface pH of the optimized formulation (F8) was found to be 4.39 ± 0.20 .

Table 4. Evaluation tests for tablet formulations Expressed as [Mean \pm SD (n=3)]

Formulation code	Physical Parameters						
	Diameter (mm)	Thickness (mm)	Hardness (Kg/cm ²)	Friability (%)	Weight variation (mg)	Drug content (%)	Surface pH
F1	12 \pm 0.31	4.98 \pm 0.21	5.52 \pm 0.26	0.52 \pm 0.30	799 \pm 0.22	97.82 \pm 0.21	4.23 \pm 0.38
F2	12 \pm 0.24	4.99 \pm 0.20	5.40 \pm 0.35	0.61 \pm 0.31	796.2 \pm 0.21	98.23 \pm 0.22	4.29 \pm 0.26
F3	12 \pm 0.33	5.00 \pm 0.25	5.67 \pm 0.36	0.32 \pm 0.28	797.1 \pm 0.29	99.03 \pm 0.32	4.38 \pm 0.20
F4	12 \pm 0.28	5.03 \pm 0.32	6.02 \pm 0.48	0.50 \pm 0.40	801.1 \pm 0.36	98.56 \pm 0.24	4.50 \pm 0.33
F5	12 \pm 0.25	5.02 \pm 0.22	6.13 \pm 0.20	0.43 \pm 0.26	798.1 \pm 0.29	96.42 \pm 0.30	4.29 \pm 0.34
F6	12 \pm 0.22	4.97 \pm 0.23	5.47 \pm 0.34	0.42 \pm 0.37	802.0 \pm 0.30	97.83 \pm 0.21	4.27 \pm 0.21
F7	12 \pm 0.21	4.98 \pm 0.20	5.42 \pm 0.22	0.52 \pm 0.22	798.1 \pm 0.26	96.63 \pm 0.23	4.25 \pm 0.22
F8	12 \pm 0.16	4.49 \pm 0.19	5.79 \pm 0.21	0.30 \pm 0.21	799.2 \pm 0.20	98.71 \pm 0.19	4.39 \pm 0.20
F9	12 \pm 0.28	5.00 \pm 0.24	5.56 \pm 0.36	0.49 \pm 0.35	797.2 \pm 0.33	96.49 \pm 0.27	4.35 \pm 0.31

Swelling Index

The swelling property of all the batches F1- F9 was determined by assessing the swelling index at different time intervals (1, 2, 3, 4 up to 8 hr) and the result was depicted in (Figure 13). The highest swelling was shown in the batch F5 and F4 i.e. 118.54 \pm 0.13 % and 110.36 \pm 0.12 % after 8 hr (480 min). Though the most reduced expanding conduct was shown by the group F7 and F6 72.54 \pm 0.44 % and 75.12 \pm 0.28 % after 8 hr (480 min). All the formulations showed a considerable increase in swelling index proportional to the time increases and maximum swelling effect occurring at 8hr (480 min). The swelling index is shown by the optimized batch F8 containing (HPMC K15M: Guar gum) in (1:7.5) ratio i.e. 86.50 \pm 0.11%. From this, it was found that the swelling index is directly proportional to the concentration of mucoadhesive polymer, as the polymer concentration increases there is an increase in the swelling index [47]. The tablet formulations F1 and F2 containing HPMCK15M and Guar gum alone showed a swelling index of 90.13 \pm 0.21 % and 102.42 \pm 0.11 % respectively. Initially, guar gum swells rapidly but when used alone was eroded faster [48]. But in combination with HPMC K15M swelling index reduced and remained intact. While the increase in HPMC K15M concentration caused a greater degree of the swelling index, HPMC K15M facilitates the formation of a protective viscous gel layer preceding section of water into the lattice ruining quick hydration of the tablet inward core due to its high viscosity and was able to maintain the integrity of the tablet [32, 49]. As a result matrix integrity, swelling process, as well as mucoadhesive properties, were all significantly influenced by the polymer's viscosity [47]. Swelling capacity is crucial because it controls the formulation's mucoadhesive property and improves adhesive material's adsorption onto the mucosa [20].

**Figure13.** % Swelling Index of mucoadhesive tablets F1 to F9

Ex vivo mucoadhesion time

Ex vivo mucoadhesion time and behavior were performed to evaluate tablet residence time onto the vaginal mucosal membrane and to observe tablet behavior in contact with the mucosal surface in the presence of phosphate buffer pH 4.5 [26]. It was observed that all of the examined tablets adhered immediately to the vaginal mucosal surface. Ex vivo mucoadhesion time for all the formulations F1-F9 varied from (10.88 \pm 0.10 to 12.02 \pm 0.13hr) as shown in (Figure 14). The difference could be due to the different amounts of mucoadhesive polymer concentration. The residence time of formulations F1, F4, F5, and F8 with vaginal mucosal tissue were

significantly longer exceeding 12 hr with the slow erosion of the compact viscous gel layer surrounding the tablet than that of formulations F3, F6, and F7. Mucoadhesion time increases as the polymer concentration increases. Optimized batch F8 showed an acceptable mucoadhesion time was 12.01 ± 0.07 hr. This is due to the high mucoadhesive nature of the combined polymers and interpenetration of the polymeric chain into the mucosal membrane [50]. Batch F1 and F2 containing HPMCK15M and Guar gum alone showed mucoadhesion times 12.02 ± 0.13 and 10.88 ± 0.10 hr. HPMCK15M showed maximum mucoadhesion time than guar gum this is because guar gum showed the highest hydration capacity. In this manner the hydrated polymer delivered on the tablet surface is presented to disintegration.

Ex vivo Mucoadhesive study (Determination of force of adhesion)

The In vitro mucoadhesion study was performed on modified physical balance and measure the force required to detach the tablet from goat vaginal mucosa and the result of the force of adhesion of all batches F1-F9 were graphically represented in (Figure 15). Mucoadhesive strength depends on the nature and different ratios of mucoadhesive polymer used in the formulation [33]. An increase in the concentration of mucoadhesive polymer greater the mucoadhesive strength and mucoadhesive force [39]. The mucoadhesive force of all formulations was found to be in the range (of 2.1 ± 0.20 N to 3.55 ± 0.39 N). The lowest value was observed in batches F7 and F6 i.e., 2.10 ± 0.20 and 2.21 ± 0.13 N, and in which the lowest proportion of polymer was incorporated. Also, batch F2 showed 2.19 ± 0.19 N force of adhesion. The possible reason was weak bond formation with mucosa. Similarly, the highest value was observed in batch F5 and F4 i.e., 3.55 ± 0.39 N and 3.41 ± 0.42 N in which the highest ratio of polymer used which sometimes leads to local irritation in the vagina. So, the optimized batch F8 showed a moderate force of adhesion i.e., 2.59 ± 0.25 N. In this study, the mucoadhesive force of formulation was observed to be prominently influenced by the concentration of mucoadhesive polymer. HPMCK15M is a long chain, a non-ionic polymer that showed maximum adhesion strength may be due to the formation of a strong hydrogen bond with mucin [39]. Hence, attachment to the mucosal layer was strong as compared to guar gum and with a combination of HPMCK15M and Guar gum improved adhesion strength by the polymer chain of the polymer interpenetrating the mucin lining of the mucosal membrane giving better mucoadhesive as compared to the alone polymer. All the formulated batches exhibited satisfactory mucoadhesive force.

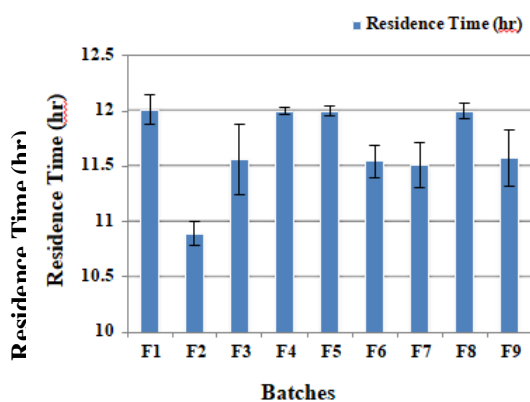


Figure 14. Residence time (hr) of mucoadhesive tablets F1-F9.

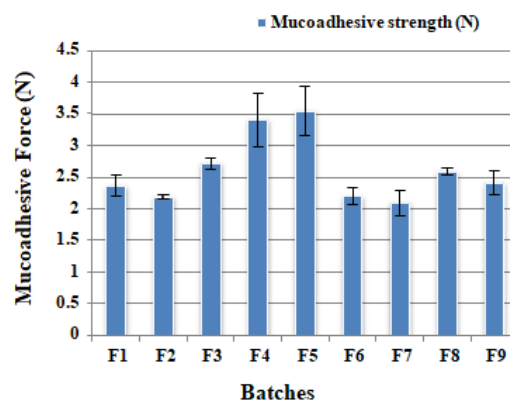


Figure 15. Mucoadhesive Force (N) of mucoadhesive tablets F1-F9.

In vitro dissolution study

The in vitro dissolution study of all the formulations F1-F9 was carried out in phosphate buffer pH 4.5 up to 12 hr (720 min). The release of SRN was monitored for tablets containing a single mucoadhesive polymer and a combination of HPMC K15M and Guar gum with different concentrations to choose the best plan with delayed discharge properties. The effect of the different ratios of polymers concentration on the dissolution of SRN from mucoadhesive vaginal tablets was shown in (Figure 16). Formulations F1 and F2 contained a single mucoadhesive polymer and showed an initial burst effect. But with a combination of HPMCK15M and Guar gum in optimum concentration, initial burst release was eliminated and the drug was released in a controlled fashion. The drug release observed in formulation F1 contained HPMC K15M was $80.16 \pm 0.32\%$ even after 12 hr (720 min) i.e., showing the slow release of the drug due to building up exorbitantly thick gel which is exceptionally impervious to water infiltration and disintegration. On the other hand tablet formulation F2 containing guar gum alone shows rapid disintegration, more erodability, and faster drug release within 7 to 8 hr (420 to 480 min) resulting in a less prolonged release. At high concentration, HPMCK15M acts as an excess release retardant. But when HPMCK15M is combined with guar gum at optimum concentration, guar gum helps for erosion and showed prolonged drug release. Formulation F3 contained (HPMCK15M: Guar gum) in (1:1) ratio showed $87.08 \pm 0.19\%$ at 12 hr (720 min). In the case of batch F4 contained (HPMCK15M: Guar gum) in

(1:2) ratio and batch F5 contained (HPMCK15M: Guar gum) in (2:1) ratio the drug release was found to be very slow even after 12 hr 720 min i.e. $74.74 \pm 0.13\%$ and $68.23 \pm 0.51\%$ which not satisfactory to achieve 100 % drug release. This might be due to the high concentration of HPMCK15M and Guar gum ratio. Thus drug release made with a higher concentration of polymer shows slower drug release. This might be due to an increase in diffusional path length [39]. Formulation F6 contained (HPMCK15M: Guar gum) in (1:0.5) ratio and F7 contained (HPMCK15M: Guar gum) in (0.5:1) ratio the drug release was found to be $93.06 \pm 0.11\%$ and $92.78 \pm 0.19\%$ at 10 hr (600 min) and 9 hr (540 min). Here percentage drug release was observed faster than the requirement, this might be due to less mucoadhesive polymer concentration. Also the formulations F8 and F9 the drug release was found to be $95.63 \pm 0.16\%$ and $90.06 \pm 0.14\%$ at 12 hr (720 min) and 10 hr (600 min). Formulation F8 contained (HPMCK15M: Guar gum) in (1:0.75) optimum ratio shows acceptable sustained drug release up to 12 hr (720 min) compare to other formulations and exactly fits the criteria for drug release. (Tablet should release more than 90% of drug within 11 hr (660 min) to 12 hr (720 min)). Whereas pure drugs release $95.29 \pm 0.23\%$ within only 4.66 hr (280 min). So on the basis of sustained and acceptable drug release and moderate mucoadhesion (2.59 ± 0.25 N), the F8 batch was selected as the optimized batch and it is a good candidate for the development of a mucoadhesive vaginal tablet containing SRN-loaded silver nanoparticles.

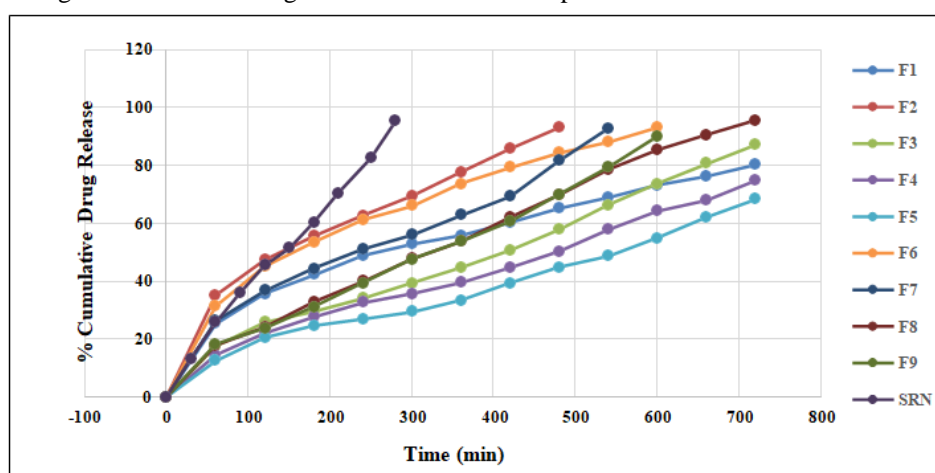


Figure 16. Dissolution drug profile of mucoadhesive tablets F1-F9 and pure drug.

Drug release kinetics

In the kinetic study, all the formulations in this investigation could be best expressed by Korsmeyer–Peppas kinetic model (their medication discharge instrument can't be depicted precisely or more than one sort of delivery is involved) [33, 47]. The release kinetics indicated that the optimized bath (F8) followed Korsmeyer Peppas kinetics where R is 0.9858, n is 0.709 and k is 15.21. All the formulations showed values ranging from ($0.45 < n < 0.89$), indicating that non-fickian diffusion or anomalous release is shown in (Table 5). ($n = 0.45$ indicates Fickian diffusion; $0.45 < n < 0.89$ indicates non-fickian diffusion). Non-fickian diffusion involves a combination of both diffusion and erosion-controlled release rate [18].

Table 5. Release kinetics of mucoadhesive tablet batches F1-F9

Batch code	Zero order model	First order model	Higuchi/Matrix model	Hixson Crowell model	Korsmeyer-Peppas mode			Best fit kinetic model
	R	R	R	R	R	n	K	
F1	0.8276	0.9761	0.9960	0.9504	0.9962	0.4488	25.29	KP
F2	0.9128	0.9659	0.9851	0.9945	0.9835	0.4882	31.95	KP
F3	0.9780	0.9456	0.9582	0.9742	0.9783	0.6363	15.70	KP
F4	0.9744	0.9805	0.9689	0.9882	0.9917	0.6466	13.63	KP
F5	0.9764	0.9755	0.9579	0.9829	0.9837	0.6481	11.86	KP
F6	0.8375	0.9887	0.9976	0.9796	0.9977	0.4656	32.04	KP
F7	0.9339	0.8969	0.9676	0.9426	0.9680	0.5352	24.56	KP
F8	0.9850	0.9087	0.9519	0.9617	0.9858	0.7090	15.21	KP
F9	0.9805	0.9092	0.9517	0.9558	0.9807	0.7013	15.51	KP

Fourier Transform Infra-Red Spectroscopy (FT-IR)

A medication excipient similarity concentrate on test was completed to really look at the connection among drugs and excipients. The FTIR spectra of SRN with polymer (physical mixture) and final tablet formulation F8

were evaluated (Figure 17, 18). The FT-IR spectra of SRN with polymer were carried out and it was found that all the peaks retained in their appropriate range and all the peaks of the pure drug were retained in a physical mixture. Hence they were compatible with each other. The FTIR spectra of the final tablet formulation containing Ser-AgNP1 (F8) were evaluated (Figure 18) which determines that all the functional group frequencies of SRN-loaded silver nanoparticles were found to be within the ranges. No change was observed, which indicated there was no interaction between SRN-loaded silver nanoparticles and the excipients this confirms the compatibility of the drug with excipients.

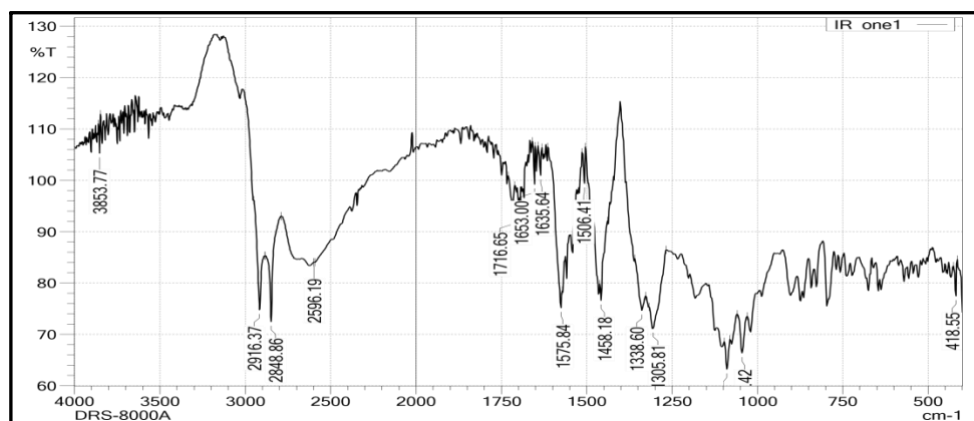


Figure 17. FT-IR spectra of SRN with polymer (physical mixture)

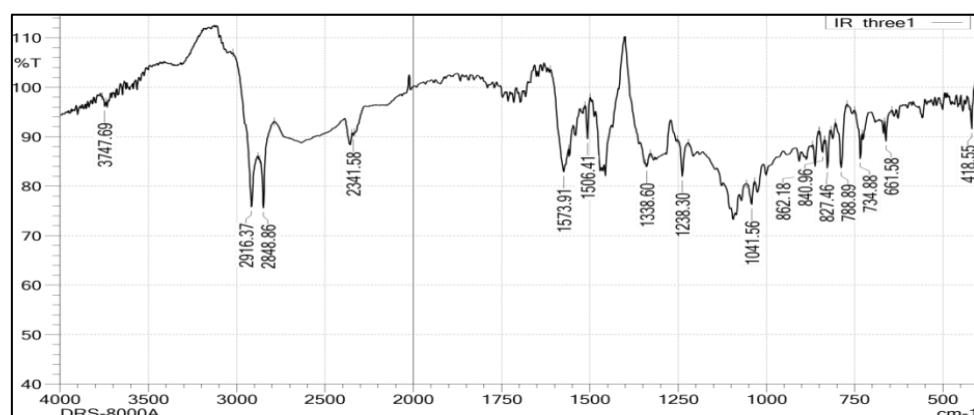


Figure 18. FT-IR spectra of final tablet formulation containing Ser-AgNP1 (F8)

Differential scanning calorimetry (DSC)

DSC thermograms demonstrated and confirmed that there was no drug-polymer interaction. The sharp endothermic peak of pure SRN and the endothermic peak of Ser- AgNP1 shows in (Figure 19) and (Figure 20) at 158.4 & 167.7°C which was due to the melting point of drug and polymer (physical mixture) and optimized tablet batch F8.

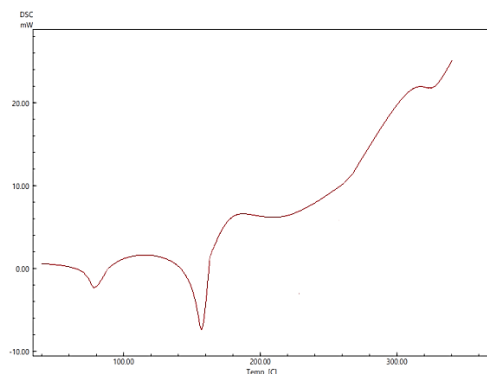


Figure 19. DSC thermogram of SRN and polymers (physical mixture)

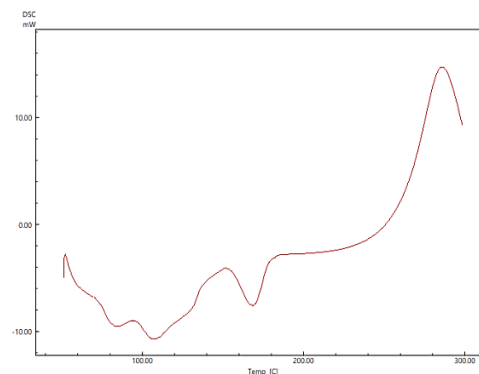


Figure 20. DSC spectra of optimized tablet batch F8

The broad peak in (Figure 19) of HPMC K15M was observed at 82.4°C (reported value 45.01-110.2°C) in a physical mixture [51], whereas in (Figure 20) HPMC K15M and Guar gum were observed at 108.8°C, 80.4°C [52], and disappearance of melting peak of guar gum in (Figure 19) and chitosan and microcrystalline cellulose in (Figure 20) this may be due to the volatilization of adsorbed water, following the melting decomposition of the polymer. This indicates the absence of Drug-Polymer interaction [51].

Antifungal study

The result of antifungal studies was shown in (figure 21) and graphically in (figure 22). The antifungal activity revealed that the formulation F8 produced the largest microbial zone of inhibition i.e., 31.71 ± 0.18 mm after 48 h incubation as compared with marketed formulations (Vaginal suppository produced zone of inhibition i.e., 23.18 ± 0.17 mm vaginal tablet produced zone of inhibition i.e. 27.69 ± 0.21 mm). The formulation F8 produced the maximum zone of inhibition due to the presence of standard drugs (SRN), silver nanoparticles, and chitosan. Where silver nanoparticles and chitosan has been proven to have antifungal activity against *C. albicans*. Silver nanoparticles and chitosan showed a zone of inhibition against *C. albicans* i.e., 16.06 ± 0.11 mm and 13.16 ± 0.13 mm respectively.

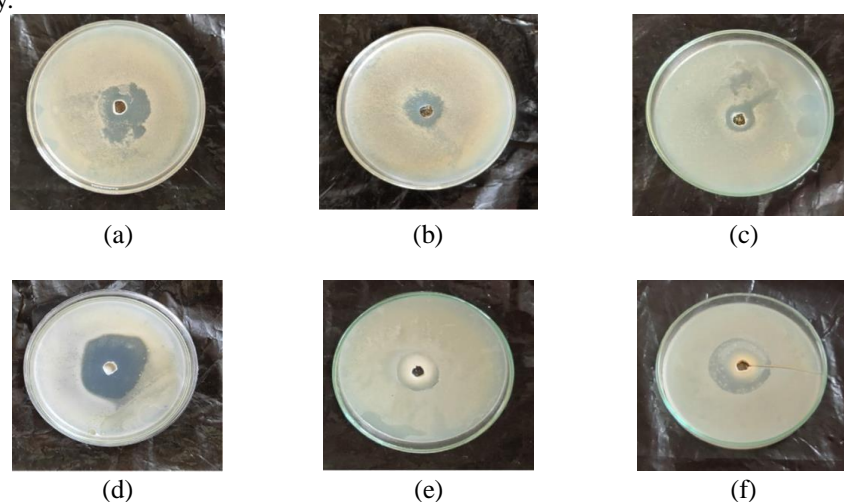


Figure 21. Figure (a) Antifungal activity of pure SRN against *candida albicans*. Figure (b) Antifungal activity of silver nanoparticles against *candida albicans*. Figure (c) Antifungal activity of chitosan against *candida albicans*. Figure (d) Antifungal activity of optimized mucoadhesive vaginal tablet (F8) against *candida albicans*. Figure (e) Antifungal activity of marketed vaginal suppository against *candida albicans*. Figure (f) Antifungal activity of marketed vaginal tablet against *candida albicans*.

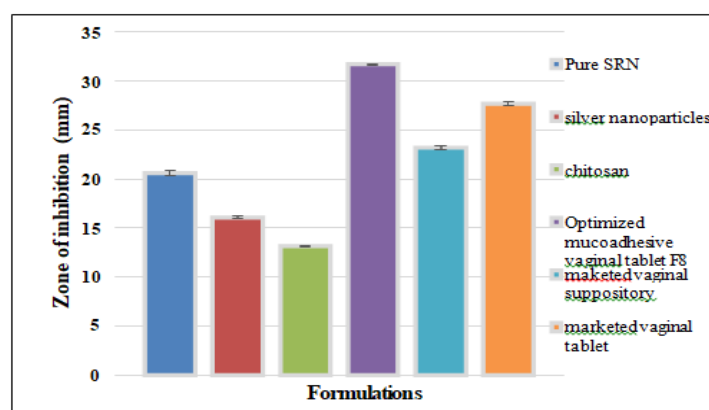


Figure 22. Graphical representation of zone of inhibition (mm) for SRN, silver nanoparticles, chitosan, optimized mucoadhesive vaginal tablet F8, marketed vaginal suppository, marketed vaginal tablet.

Stability studies

Optimized batch F8 was selected for the stability study. A stability study of tablets was carried out at room temperature ($25 \pm 2^\circ\text{C}$) and at accelerated conditions ($40 \pm 2^\circ\text{C}$ & $75 \pm 5\%$ RH) for 3 months shown in (Table 6). The sample was withdrawn after 1 month, 2 months, and 3 months. The results obtained showed no significant difference in % drug content, mucoadhesive strength (N), % swelling index, and in vitro cumulative percentage

of drug release %. So, it can be predicted that the developed formulation retained good stability under these storage conditions for at least 3 months.

Table 6. Stability study of optimized formulation (F8)

Time Period	Swelling index (%)		Mucoadhesive force (N)		Drug content (%)		Cumulative drug release (%) 12 hr	
	Room temperature (25±2°C)	Accelerated (40±2°C & 75 ± 5 % RH)	Room temperature (25± 2°C)	Accelerated (40±2°C & 75 ± 5% RH)	Room temperature (25±2°C)	Accelerated (40±2°C & 75 ± 5% RH)	Room temperature (25±2°C)	Accelerated (40±2°C & 75 ± 5% RH)
0 Day	86.50±0.11	86.50±0.11	2.59±0.25	2.59±0.25	98.71±0.13	98.71±0.13	95.63±0.16	95.63±0.16
After 1 month	86.59±0.14	86.72±0.13	2.60±0.10	2.51±0.12	98.70±0.24	98.65±0.11	95.52±0.28	95.34±0.13
After 2 month	86.89±0.18	86.39±0.21	2.49±0.16	2.32±0.17	98.62±0.31	98.41±0.23	95.38±0.08	94.99±0.27
After 3 month	86.82±0.22	87.07±0.12	2.45±0.20	2.39±0.15	98.69±0.05	98.32±0.27	94.12±0.32	94.68±0.04

Conclusion

The present study successfully synthesized SRN loaded silver nanoparticles with chitosan as a stabilizer by chemical reduction method. The synthesis of silver nanoparticle is confirmed by UV-visible spectroscopy at surface plasmon resonance peak 401.5±0.38 nm. The linkage between SRN and silver nanoparticles was confirmed by FT-IR. The SEM revealed irregular morphology with slight aggregation of Ser-AgNP1. The saturationsolubility of the Ser-AgNP1 was found to be increased by 2.51 folds as compared with pure drug. In the study mucoadhesive vaginal tablets containing Ser-AgNP1 was formulated and evaluated which gives sustained release property to achieve patient compliance by achieving high drug level at the target site, reduction of repeated daily administration of dose and side effect minimization. The results show that selected HPMC K15M and Guar gum combination at optimum concentration successfully developed the sustained release mucoadhesive vaginal tablet for local treatment of vaginal candidiasis. Optimized formulation shows the larger antifungal activity against *Candida albicans* as compare to SRN marketed formulations which may be due to SRN in silver nanoparticles and presence of chitosan.

Funding

This research received no external funding.

Acknowledgments- Nil

Conflicts of Interest

The authors have no conflicts of interest regarding this investigation.

References

- [1] Gagandeep, Garg T, Malik B, Rath G, Goyal AK. Development and characterization of nano-fiber patch for the treatment of glaucoma. *European Journal of Pharmaceutical Sciences*. **2014**;53:10-16. doi:10.1016/j.ejps.2013.11.016
- [2] Pérez-González N, Bozal-de Febrer N, Calpena-Campmany AC, Nardi-Ricart A, Rodríguez-Lagunas MJ, Morales-Molina JA, Soriano-Ruiz JL, Fernández-Campos F, Clares-Naveros B. New Formulations Loading Caspofungin for Topical Therapy of Vulvovaginal Candidiasis. *Gels*. **2021**;7(4):259. doi:10.3390/gels7040259
- [3] Martínez-Pérez B, Quintanar-Guerrero D, Tapia-Tapia M, Cisneros-Tamayo R, Zambrano-Zaragoza ML, Alcalá-Alcalá S, Mendoza-Muñoz N, Piñón-Segundo E. Controlled-release biodegradable nanoparticles: From preparation to vaginal applications. *European Journal of Pharmaceutical Sciences*. **2018**;115:185-195. doi:10.1016/j.ejps.2017.11.029
- [4] Abdellatif MM, Khalil IA, Elakkad YE, Eliwa HA, Samir TM, Al-Mokaddem AK. Formulation and Characterization of Sertaconazole Nitrate Mucoadhesive Liposomes for Vaginal Candidiasis. *Int J Nanomedicine*. **2020** Jun 11;15:4079-4090. doi: 10.2147/IJN.S250960.
- [5] Samrat K, Nikhil N, Karthick Raja Namasivamyam S, Sharath R, Chandraprabha M, Harish B, Muktha H, Kashyap RG. Evaluation of improved antifungal activity of fluconazole- silver nanoconjugate against pathogenic fungi. *Materials Today: Proceedings*. **2016**;3(6):1958-

- 1967.doi:10.1016/j.matpr.2016.04.097
- [6] Galatage S, Hebalkar A, Dhobale S, Mali O, Kumbhar P, Nikade S, Killedar S. Silver Nanoparticles: Properties, Synthesis, Characterization, Applications and Future Trends. *Silver Micro-Nanoparticle*. **2021**. doi:10.5772/intechopen.99173
- [7] Shanmugam R, Madhuri K, Dwarampudi LP, Bhaskaran M, Kongara D, Tesfaye JL, Nagaprasad N, Bhargavi VLN, Krishnaraj R. Review on silver nanoparticle synthesis method, antibacterial activity, drug delivery vehicles, and toxicity pathways: Recent advances and future aspects. *Journal of Nanomaterials*. **2021**;1-11. doi:10.1155/2021/4401829
- [8] Byrne McDonnell S, Gunes S, Casey A, F Curtin J, Manaloto E. Synthesis and Characterization of Silver Nanoparticles using Sodium Borohydride as a Reducing Agent v1. **2021**.doi:10.17504/protocols.io.buq4nvyw
- [9] Samiyah Saeed Al-Zahrani, Roop Singh Bora & Saleh Mohammed Al-Garni. Antimicrobial activity of chitosan nanoparticles, *Biotechnology & Biotechnological Equipment*. **2021**; 35:1, 1874- 1880, DOI: 10.1080/13102818.2022.2027816
- [10] Pansara C, Chan WY, Parikh A, Trott DJ, Mehta T, Mishra R, Garg S. Formulation optimization of chitosan-stabilized silver nanoparticles using in vitro antimicrobial assay. *Journal of Pharmaceutical Sciences*. **2019**;108(2):1007-1016. doi:10.1016/j.xphs.2018.09.011
- [11] Croxtall JD, Plosker GL. Sertaconazole. *Drugs*. 2009;69(3):339-359. doi:10.2165/00003495-200969030-00009
- [12] Arsha G, Naseeb S, PK Lakshmi and Latha K. Formulation and Evaluation of Sertaconazole nitrate loaded Nanosponges for topical application. *Research J. Pharm. and Tech*. **2021**; 14(2):895-902. doi: 10.5958/0974-360X.2021.00159.1
- [13] Carrillo-Muñoz AJ, Tur-Tur C, Giusiano G, et al. Sertaconazole: an antifungal agent for the topical treatment of superficial candidiasis. *Expert Rev Anti Infect Ther*. 2013;11(4):347-358. doi: 10.1586/eri.13.17
- [14] Alawdi S, Solanki AB. Mucoadhesive Drug Delivery Systems: A Review of Recent Developments. *Journal of Scientific Research in Medical and Biological Sciences*. 2021;2(1):50-64. doi:10.47631/jsrmb.v2i1.213Mahours G, Ali Sherif A. "formulation and evaluation of fluconazole muco-adhesive vaginal tablets". *British Journal of Pharmaceutical Research*. December 2016;14(2):1-10. doi:10.9734/BJPR/2016/30629
- [15] Pansara C, Mishra R, Mehta T, Parikh A, Garg S. Formulation of chitosan stabilized silver nanoparticle-containing wound healing film: in vitro and in vivo characterization. *Journal of Pharmaceutical Sciences*. **2020**;109(7):2196-2205. doi:10.1016/j.xphs.2020.03.028
- [16] Kumar CG, Poornachandra Y. Biodirected synthesis of miconazole-conjugated bacterial silver nanoparticles and their application as antifungal agents and drug delivery vehicles. *Colloids and Surfaces B: Biointerfaces*. 2015;125:110-119. doi:10.1016/j.colsurfb.2014.11.025
- [17] Chaudhari PD, Desai US. Formulation and evaluation of niosomal in situ gel of prednisolone sodium phosphate for ocular drug delivery. *International Journal of Applied Pharmaceutics*. 2019;97-116. doi:10.22159/ijap.2019v11i2.30667
- [18] Jackson T, Patani B. Development of Metronidazole Loaded Silver Nanoparticles from *Acalypha ciliata* for Treatment of Susceptible Pathogens. *Nanoscience and Nanotechnology*. 2019;9(1):22-28. doi:DOI: 10.5923/j.nn.20190901.02
- [19] Rao MR, Paul G. Vaginal delivery of clotrimazole by mucoadhesion for treatment of candidiasis. *Journal of Drug Delivery and Therapeutics*. 2021;11(6):6-14. doi:10.22270/jddt.v11i6.5116
- [20] Nair SC, Kumar BS, Krishna R, Ps L, Vasudev DT. Formulation and evaluation of niosomal suspension of cefixime. *Asian Journal of Pharmaceutical and Clinical Research*. 2017;10(5):194. doi:10.22159/ajpcr.2017.v10i5.17189
- [21] Hussein-Al-Ali SH, Abudoleh SM, Abualassal QIA, Abudayeh Z, Aldalhamah Y, Hussein MZ. Preparation and characterisation of ciprofloxacin-loaded silver nanoparticles for drug delivery. *IET Nanobiotechnology*. 2022;16(3):92-101. doi:10.1049/nbt2.12081
- [22] Kadnor N, Pande V, Kadam R, Upadhye S. Fabrication and characterization of sertaconazole nitrate microsphere as a topical drug delivery system. *Indian Journal of Pharmaceutical Sciences*. 2015;77(6):675. doi:10.4103/0250-474x.174986
- [23] Sanjeevani Deshkar, Harshad Kapare, Shramika Chore, Anjali Thakre, Jayashri Mahore. Formulation Development and evaluation of mucoadhesive tablets for vaginal delivery of metronidazole. *International Journal of Research in Pharmaceutical Sciences*. 2020;11:1973-1981. doi:10.26452/ijrps.v11i19pl4.4535
- [24] Garg S, Garg A. Encapsulation of curcumin in silver nanoparticle for enhancement of anticancer drug delivery. *International Journal of Pharmaceutical Sciences and Research*. 2018;9(3):1160-1166. doi:10.13040/IJPSR.0975-8232.9(3).1160-66
- [25] Fitaihi RA, Aleanizy FS, Elsamaligy S, Mahmoud HA, Bayomi MA. Role of chitosan on controlling the characteristics and antifungal activity of bioadhesive fluconazole vaginal tablets. *Saudi Pharmaceutical Journal*.

- 2018;26(2):151-161. doi:10.1016/j.jsps.2017.12.016
- [26] Anepu S, Duppala L. Formulation development, characterization and in- vitro evaluation of floating matrix dosage form of tramadol hydrochloride using various polymers. *Asian Journal of Pharmaceutical and Clinical Research*. 2017;10(2):281. doi:10.22159/ajpcr.2017.v10i2.15587
- [27] Shakir R, Hanif S, Salawi A, Arshad R, Sarfraz RM, Irfan M, Raza SA, Barkat K, Sabei FY, Almoshari Y, Alshamrani M, Syed MA. Exorbitant Drug Loading of Metformin and Sitagliptin in Mucoadhesive Buccal Tablet: In Vitro and In Vivo Characterization in Healthy Volunteers. *Pharmaceuticals*. 2022;15(6):686. doi:10.3390/ph15060686
- [28] Gupta NV, Natasha S, Getyala A, Bhat RS. Bioadhesive vaginal tablets containing spray dried microspheres loaded with clotrimazole for treatment of vaginal Candidiasis. *Acta Pharmaceutica*. 2013;63(3):359-372. doi:10.2478/acph-2013-0027
- [29] Li KL, Castillo AL. Formulation and evaluation of a mucoadhesive buccal tablet of mefenamic acid. *Brazilian Journal of Pharmaceutical Sciences*. 2020;56. doi:10.1590/s2175-97902019000418575
- [30] Lalwani PM, Barhate S, Bari M. Formulation and evaluation of mucoadhesive tablet of ondansetron hcl. *Asian Journal of Pharmacy and Technology*. 2018;8(3):132. doi:10.5958/2231-5713.2018.00021.1
- [31] Preetha P, Srinivasa rao A, BanutejaNaik B. Formulation and evaluation of stavudineas mucoadhesive vaginal tablets. *International Journal of Pharmaceutical Sciences and Research*. February 2015;6(2):928- 934. doi:10.13040/IJPSR.0975-8232.6 (2).
- [32] Koirala S, Nepal P, Ghimire G, Basnet R, Rawat I, Dahal A, Pandey J, Parajuli-Baral K. Formulation and evaluation of mucoadhesive buccal tablets of aceclofenac. *Heliyon*. 2021;7(3). doi:10.1016/j.heliyon.2021.e06439
- [33] Mohite B, Patel R, Kayande N, Thenge R. Vaginal Mucoadhesive Drug Delivery System. *Journal of Pharmaceutical Research International*. 2021;123-133. doi:10.9734/jpri/2021/v33i51a33476.
- [34] Hani U, Shivakumar H, Osmani R. Development of a curcumin bioadhesive monolithic tablet for treatment of vaginal candidiasis. *Iranian Journal of Pharmaceutical Research* . 2016;15(1):23-34.
- [35] Patel A, Patel K, Patel DJ. Development and evaluation of mucoadhesive vaginal tablet of sertaconazole for vaginal candidiasis. *International Journal of PharmTech Research*.2011;3(4):2175- 2182. www.researchgate.net/publication/266588229.
- [36] Boddu P, Mudili NR, Ponokumati UD. Formulation development and optimization of press coated tablets of ranitidine hcl by using 32 factorial design. *Jordan Journal of Pharmaceutical Sciences*. 2017;10(1):57- 75. doi:10.12816/0039542
- [37] Patel VM, Prajapati BG, Patel MM. Formulation, evaluation, and comparison of bilayered and multilayered mucoadhesive buccal devices of propranolol hydrochloride. *AAPS PharmSciTech*.2007;8(1). doi:10.1208/pt0801022
- [38] Bhat S, Shivakumar H. Bioadhesive controlled release clotrimazole vaginal tablets. *Tropical Journal of Pharmaceutical Research*. 2010;9(4). doi:10.4314/tjpr.v9i4.58924
- [39] Kanojia D, Patel D. Formulation and evaluation of mucoadhesive vaginal tablet for the treatment of bacterial vaginosis. *International Journal of Pharmaceutical Sciences and Research*. 2021;12(4):2320-5148. doi:10.13040/IJPSR.0975-8232.12(4).2330-37
- [40] Desai R, Mankad V, Gupta S, Jha P. Size distribution of silver nanoparticles: uv-visible spectroscopic assessment. *Nanoscience and Nanotechnology Letters*. 2012;4(1):30-34. doi:10.1166/nnl.2012.1278
- [41] Hien LT, Hue NTP, Duc LT, Huyen VT, Van LT, Giang HT, Ha CD, Ha NT, Phuong ND, Ham LH. Synthesis of chitosan stabilized silver nanoparticles and evaluation of the in vitro antibacterial activity against xanthomonas oryzae pv. Oryzae causing blight disease of rice. *VNU Journal of Science: Natural Sciences and Technology*. 2021. doi:10.25073/2588-1140/vnunst.5223
- [42] Pande V. Design and synthesis of mesoporous silica for inclusion of poorly water soluble drug sertaconazole nitrate as a drug delivery platform. *Scholar Research Library*. February 2014;6(4):159-168. www.researchgate.net/publication/279837429.
- [43] Zhao L, Duan X, Cao W, Ren X, Ren G, Liu P, Chen J. Effects of Different Drying Methods on the Characterization, Dissolution Rate and Antioxidant Activity of Ursolic Acid-Loaded Chitosan Nanoparticles. *Foods*. 2021;10(10):2470. doi:10.3390/foods10102470
- [44] Laghrib F, Ajermoun N, Bakasse M, Lahrich S, El Mhammedi M. Synthesis of silver nanoparticles assisted by chitosan and its application to catalyze the reduction of 4-nitroaniline. *International Journal of Biological Macromolecules*. 2019;135:752-759. doi:10.1016/j.ijbiomac.2019.05.209
- [45] Lin YP, Chen WC, Cheng CM, Shen CJ. Vaginal pH Value for Clinical Diagnosis and Treatment of Common Vaginitis. *Diagnostics (Basel)*.2021 Oct 27;11(11):1996. doi: 10.3390/diagnostics11111996.
- [46] Patil P, Kulkarni S, Ammanage A. Formulation and in vitro evaluation of mucoadhesive tablets of ofloxacin using natural gums. *International Journal of Current Pharmaceutical Research*.2011;3(2):93- 98.

- [46] Dalvadi HP. Development and characterization of controlled release mucoadhesive tablets of captopril to increase the residence time in the gastrointestinal tract. *Latin American Journal of Pharmacy*. April 2011;30(2):266-272. www.researchgate.net/publication/259998819.
- [47] Mughal MA, Iqbal Z, Neau SH. Guar gum, xanthan gum, and hpmc can define release mechanisms and sustain release of propranolol hydrochloride. *AAPS PharmSciTech*. 2010;12(1):77-87. doi:10.1208/s12249-010-9570-1
- [48] Singh S, Goswami H. Formulation of oral mucoadhesive tablets of pioglitazone using natural gum from seeds of *pithecellobium dulce*. *International Journal of Pharmaceutical Sciences and Nanotechnology*. 2015;8(4):3031-3038. doi:10.37285/ijpsn.2015.8.4.6
- [49] El-Masry SM, Helmy SA. Hydrogel-based matrices for controlled drug delivery of etamsylate: prediction of in-vivo plasma profiles. *Saudi Pharmaceutical Journal*. 2020;28(12):1704-1718. doi:10.1016/j.jsps.2020.10.016
- [50] Kumar A, DE A, Mozumdar S. Synthesis of acrylate guar-gum for delivery of bio-active molecules. *Bulletin of Materials Science*. 2015;38(4):1025-1032. doi:10.1007/s12034-015-0930-z.